Jump Markov models and transition state theory: the Quasi-Stationary Distribution approach

Giacomo Di Gesù[a], Tony Lelièvre[*a], Dorian Le Peutrec[a,b] and Boris Nectoux[a]

We are interested in the connection between a metastable continuous state space Markov process (satisfying *e.g.* the Langevin or overdamped Langevin equation) and a jump Markov process in a discrete state space. More precisely, we use the notion of quasi-stationary distribution within a metastable state for the continuous state space Markov process to parametrize the exit event from the state. This approach is useful to analyze and justify methods which use the jump Markov process underlying a metastable dynamics as a support to efficiently sample the state-to-state dynamics (accelerated dynamics techniques). Moreover, it is possible by this approach to quantify the error on the exit event when the parametrization of the jump Markov model is based on the Eyring-Kramers formula. This therefore provides a mathematical framework to justify the use of transition state theory and the Eyring-Kramers formula to build kinetic Monte Carlo or Markov state models.

1 Introduction and motivation

Many theoretical studies and numerical methods in materials science[1], biology[2] and chemistry, aim at modelling the dynamics at the atomic level as a jump Markov process between states. Our objective in this article is to discuss the relationship between such a mesoscopic model (a Markov process over a discrete state space) and the standard microscopic full-atom description (typically a Markov process over a continuous state space, namely a molecular dynamics simulation).

The objectives of a modelling using a jump Markov process rather than a detailed microscopic description at the atomic level are numerous. From a modelling viewpoint, new insights can be gained by building coarse-grained models, that are easier to handle. From a numerical viewpoint, the hope is to be able to build the jump Markov process from short simulations of the full-atom dynamics. Moreover, once the parametrization is done, it is possible to simulate the system over much longer timescales than the time horizons attained by standard molecular dynamics, either by using directly the jump Markov process, or as a support to accelerate molecular dynamics[3–5]. It is also possible to use dedicated algorithms to extract from the graph associated with the jump Markov process the most important features of the dynamics (for example quasi-invariant sets and essential timescales using large deviation theory[6]), see for example[7,8].

In order to parametrize the jump Markov process, one needs to define rates from one state to another. The concept of jump rate between two states is one of the fundamental notions in the modelling of materials. Many papers have been devoted to the rigorous evaluation of jump rates from a full-atom description. The most famous formula is probably the rate derived in the harmonic transition state theory[9–15], which gives an explicit expression for the rate in terms of the underlying potential energy function (see the Eyring-Kramers formula (7) below). See for example the review paper[16].

Let us now present the two models: the jump Markov model, and the full-atom model, before discussing how the latter can be related to the former.

1.1 Jump Markov models

Jump Markov models are continuous-time Markov processes with values in a discrete state space. In the context of molecular modelling, they are known as Markov state models[2,17] or kinetic Monte Carlo models[1]. They consist of a collection of states that we can assume to be indexed by integers, and rates $(k_{i,j})_{i \neq j \in \mathbb{N}}$ which are associated with transitions between these states. For a state $i \in \mathbb{N}$, the states j such that $k_{i,j} \neq 0$ are the neighboring states of i denoted in the following by

$$\mathcal{N}_i = \{ j \in \mathbb{N}, k_{i,j} \neq 0 \}. \tag{1}$$

[a] CERMICS, École des Ponts, Université Paris-Est, INRIA, 77455 Champs-sur-Marne, France. E-mail: {di-gesug,lelievre,nectoux}@cermics.enpc.fr

[b] Laboratoire de Mathématiques d'Orsay, Univ. Paris-Sud, CNRS, Université Paris-Saclay, 91405 Orsay, France. E-mail: dorian.lepeutrec@math.u-psud.fr

[*] Corresponding author.

One can thus think of a jump Markov model as a graph: the states are the vertices, and an oriented edge between two vertices i and j indicates that $k_{i,j} \neq 0$.

Starting at time 0 from a state $Y_0 \in \mathbb{N}$, the model consists in iterating the following two steps over $n \in \mathbb{N}$: Given Y_n,

- Sample the residence time T_n in Y_n as an exponential random variable with parameter $\sum_{j \in \mathcal{N}_{Y_n}} k_{Y_n,j}$:

$$\forall t \geq 0, \mathbb{P}(T_n \geq t | Y_n = i) = \exp\left(-\left[\sum_{j \in \mathcal{N}_i} k_{i,j}\right] t\right). \quad (2)$$

- Sample independently from T_n the next visited state Y_{n+1} starting from Y_n using the following law

$$\forall j \in \mathcal{N}_i, \mathbb{P}(Y_{n+1} = j | Y_n = i) = \frac{k_{i,j}}{\sum_{j \in \mathcal{N}_i} k_{i,j}}. \quad (3)$$

The associated continuous-time process $(Z_t)_{t \geq 0}$ with values in $\mathbb{N}$ defined by:

$$\forall n \geq 0, \forall t \in \left[\sum_{m=0}^{n-1} T_m, \sum_{m=0}^{n} T_m\right), \quad Z_t = Y_n \quad (4)$$

(with the convention $\sum_{m=0}^{-1} = 0$) is then a (continous-time) jump Markov process.

1.2 Microscopic dynamics

At the atomic level, the basic ingredient is a potential energy function $V : \mathbb{R}^d \to \mathbb{R}$ which to a set of positions of atoms in $x \in \mathbb{R}^d$ (the dimension d is typically 3 times the number of atoms) associates an energy $V(x)$. In all the following, we assume that V is a smooth Morse function: for each $x \in \mathbb{R}^d$, if x is a critical point of V (namely if $\nabla V(x) = 0$), then the Hessian $\nabla^2 V(x)$ of V at point x is a non-singular matrix. From this function V, dynamics are built such as the Langevin dynamics:

$$dq_t = M^{-1} p_t \, dt$$
$$dp_t = -\nabla V(q_t) \, dt - \gamma M^{-1} p_t \, dt + \sqrt{2\gamma\beta^{-1}} dW_t \quad (5)$$

or the overdamped Langevin dynamics:

$$dX_t = -\nabla V(X_t) \, dt + \sqrt{2\beta^{-1}} dW_t. \quad (6)$$

Here, $M \in \mathbb{R}^{d \times d}$ is the mass matrix, $\gamma > 0$ is the friction parameter, $\beta^{-1} = k_B T > 0$ is the inverse temperature and $W_t \in \mathbb{R}^d$ is a d-dimensional Brownian motion. The Langevin dynamics gives the evolution of the positions $q_t \in \mathbb{R}^d$ and the momenta $p_t \in \mathbb{R}^d$. The overdamped Langevin dynamics is in position space: $X_t \in \mathbb{R}^d$. The overdamped Langevin dynamics is derived from the Langevin dynamics in the large friction limit and using a rescaling in time: assuming $M = \text{Id}$ for simplicity, in the limit $\gamma \to \infty$, $(q_{\gamma t})_{t \geq 0}$ converges to $(X_t)_{t \geq 0}$ (see for example Section 2.2.4 in [18]).

1.3 From a microscopic dynamics to a jump Markov dynamics

Let us now discuss how one can relate the microscopic dynamics (5) or (6) to the jump Markov model (4). The basic observation which justifies why this question is relevant is the following. It is observed that, for applications in biology, material sciences or chemistry, the microscopic dynamics (5) or (6) are metastable. This means that the stochastic processes $(q_t)_{t \geq 0}$ or $(X_t)_{t \geq 0}$ remain trapped for a long time in some region of the configurational space (called a metastable region) before hopping to another metastable region. Because the system remains for very long times in a metastable region before exiting, the hope is that it loses the memory of the way it enters, so that the exit event from this region can be modelled as one move of a jump Markov process such as (4).

Let us now consider a subset $S \subset \mathbb{R}^d$ of the configurational space for the microscopic dynamics. Positions in S are associated with one of the discrete state in $\mathbb{N}$ of $(Z_t)_{t \geq 0}$, say the state 0 without loss of generality. If S is metastable (in a sense to be made precise), it should be possible to justify the fact that the exit event can be modeled using a jump Markov process, and to compute the associated exit rates $(k_{0,j})_{j \in \mathcal{N}_0}$ from the state 0 to the neighboring states using the dynamics (5) or (6). The aim of this paper is precisely to discuss these questions and in particular to prove rigorously under which assumption the Eyring-Kramers formula can be used to estimate the exit rates $(k_{0,j})_{j \in \mathcal{N}_0}$, namely:

$$\forall j \in \mathcal{N}_0, k_{0,j} = \nu_{0,j} \exp(-\beta[V(z_j) - V(x_1)]) \quad (7)$$

where $\nu_{0,j} > 0$ is a prefactor, $x_1 = \arg\min_{x \in S} V(x)$ and $z_j = \arg\min_{z \in \partial S_j} V(z)$ where $\partial S_j \subset \partial S$ denotes the part of the boundary ∂S which connects the state S (numbered 0) with the subset of $\mathbb{R}^d$ associated with state numbered $j \in \mathcal{N}_0$. See Figure 1.
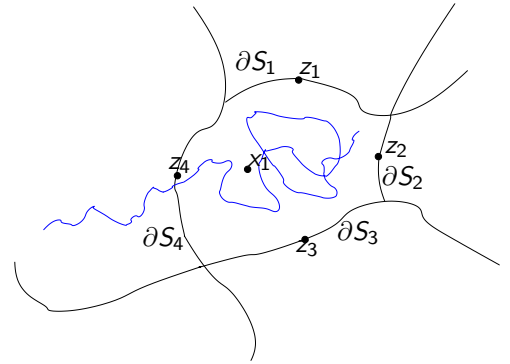

Fig. 1 The domain S. The boundary ∂S is divided into 4 subdomains $(\partial S_i)_{1 \leq i \leq 4}$, which are the common boundaries with the neighboring states.

The prefactor $\nu_{0,j}$ depends on the dynamic under consideration and on V around x_1 and z_j. Let us give a few examples. If S is taken as the basin of attraction of x_1 for the dynamics $\dot{x} = -\nabla V(x)$ so that the points z_j are order one saddle points, the prefactor writes for the Langevin dynamics (5) (assuming again $M = \text{Id}$ for

2

simplicity):

$$v_{0,j}^L = \frac{1}{4\pi} \left(\sqrt{\gamma^2 + 4|\lambda^-(z_j)|} - \gamma \right) \frac{\sqrt{\det(\nabla^2 V)(x_1)}}{\sqrt{|\det(\nabla^2 V)(z_j)|}} \qquad (8)$$

where, we recall, $\nabla^2 V$ is the Hessian of V, and $\lambda^-(z_j)$ denotes the negative eigenvalue of $\nabla^2 V(z_j)$. This formula was derived by Kramers in[14] in a one-dimensional situation. The equivalent formula for the overdamped Langevin dynamics (6) is:

$$v_{0,j}^{OL} = \frac{1}{2\pi} |\lambda^-(z_j)| \frac{\sqrt{\det(\nabla^2 V)(x_1)}}{\sqrt{|\det(\nabla^2 V)(z_j)|}}. \qquad (9)$$

Notice that $\lim_{\gamma \to \infty} \gamma v_{0,j}^L = v_{0,j}^{OL}$, as expected from the rescaling in time used to go from Langevin to overdamped Langevin (see Section 1.2). The formula (9) has again been obtained by Kramers in[14], but also by many authors previously, see the exhaustive review of the literature reported in[16]. In Section 4.1 below, we will review mathematical results where formula (8)–(9) are rigorously derived.

In practice, there are thus two possible approaches to determine the rates $(k_{i,j})$. On the one hand, when the number of states is not too large, one can precisely study the transitions between metastable states for the microscopic dynamics using dedicated algorithms[19,20]: the nudged elastic band[21], the string method[22,23] and the max flux approach[24] aim at finding one typical representative path. Transition path sampling methods[25,26] sample transition paths starting from an initial guessed trajectory, and using a Metropolis Hastings algorithm in path space. Other approaches aim at sampling the ensemble of paths joining two metastable states, without any initial guess: see the Adaptive Multilevel Splitting method[27,28], transition interface sampling[29,30], forward flux sampling[31,32], milestoning techniques[33–35] and the associated Transition Path Theory which gives a nice mathematical framework[36–38]. On the other hand, if the number of states is very large, it may be too cumbersome to sample all the transition paths, and one can use instead the Eyring-Kramers formula (7), which requires to look for the local minima and the order one saddle points of V, see for example[7]. Algorithms to look for saddle points include the dimer method[39,40], activation relaxation techniques[41,42], or the gentlest ascent dynamics[43], for example.

The aim of this paper is threefold. First, we would like to give a mathematical setting to quantify the metastability of a domain $S \subset \mathbb{R}^d$ for a microscopic dynamics such as (5) or (6), and to rigorously justify the fact that for a metastable domain, the exit event can be modeled using a jump process such as (4). This question is addressed in Section 2, where we introduce the notion of quasi-stationary distribution. Second, we explain in Section 3 how this framework can be used to analyze algorithms which have been proposed by A.F. Voter, to accelerate the sampling of the state-to-state dynamics using the underlying jump Markov process. We will discuss in particular the Parallel Replica algorithm[4]. Both these aspects were already presented by the second author in previous works, see for example the review paper[44]. The main novelty of this article is in Section 4, which is devoted to a justi-

fication of the use of the Eyring-Kramers formula (7) in order to parametrize jump Markov models.

Before getting to the heart of the matter, let us make two preliminary remarks. First, the objective of this paper is to give a self-contained overview of the interest of using the quasi-stationary distribution to analyze metastable processes. For the sake of conciseness, we therefore do not provide extensive proofs of the results we present, but we give the relevant references when necessary. Second, we will concentrate in the following on the overdamped Langevin dynamics (6) when presenting mathematical results. All the algorithms presented below equally apply to (and are actually used on) the Langevin dynamics (5). As will be explained below, the notion of quasi-stationary distribution which is the cornerstone of our analysis is also well defined for Langevin dynamics. However, the mathematical analysis of Section 4 is for the moment restricted to the overdamped Langevin dynamics (6).

2 Metastable state and quasi-stationary distribution

The setting in this section is the following. We consider the overdamped Langevin dynamics (6) for simplicity* and a subset $S \subset \mathbb{R}^d$ which is assumed to be bounded and smooth. We would like to first characterize the fact that S is a metastable region for the dynamics. Roughly speaking, metastability means that the local equilibration time within S is much smaller than the exit time from S. In order to approximate the original dynamics by a jump Markov model, we need such a separation of timescales (see the discussion in Section 3.4 on how to take into account non-Markovian features). Our first task is to give a precise meaning to that. Then, if S is metastable, we would like to study the exit event from S, namely the exit time and the exit point from S, and to see if it can be related to the exit event for a jump Markov model (see (2)–(3)). The analysis will use the notion of quasi-stationary distribution (QSD), that we now introduce.

2.1 Definition of the QSD

Consider the first exit time from S:

$$\tau_S = \inf\{t \geq 0, X_t \notin S\},$$

where $(X_t)_{t \geq 0}$ follows the overdamped Langevin dynamics (6).

A probability measure v_S with support in S is called a QSD for the Markov process $(X_t)_{t \geq 0}$ if and only if

$$v_S(A) = \frac{\int_S \mathbb{P}^x(X_t \in A, t < \tau_S) \, v_S(dx)}{\int_S \mathbb{P}^x(t < \tau_S) \, v_S(dx)}, \quad \forall t > 0, \forall A \subset S. \qquad (10)$$

Here and in the following, $\mathbb{P}^x$ denotes the probability measure under which $X_0 = x$. In other words, v_S is a QSD if, when X_0 is distributed according to v_S, the law of X_t, conditional on $(X_s)_{0 \leq s \leq t}$ remaining in the state S, is still v_S, for all positive t.

The QSD satisfies three properties which will be crucial in the

---

following. We refer for example to[46] for detailed proofs of these results and to[47] for more general results on QSDs.

2.2 First property: definition of a metastable state

Let $(X_t)_{t \geq 0}$ follow the dynamics (6) with an initial condition X_0 distributed according to a distribution μ_0 with support in S. Then there exists a probability distribution ν_S with support in S such that, for any initial distribution μ_0 with support in S,

$$\lim_{t \to \infty} \text{Law}(X_t | \tau_S > t) = \nu_S. \qquad (11)$$

The distribution ν_S is the QSD associated with S.

A consequence of this proposition is the existence and uniqueness of the QSD. The QSD is the long-time limit of the law of the (time marginal of the) process conditioned to stay in the state S: it can be seen as a 'local ergodic measure' for the stochastic process in S.

This proposition gives a first intuition to properly define a metastable state. A metastable state is a state such that the typical exit time is much larger than the local equilibration time, namely the time to observe the convergence to the QSD in (11). We will explain below how to quantify this timescale discrepancy (see (15)) by identifying the rate of convergence in (11) (see (14)).

2.3 Second property: eigenvalue problem

Let $L = -\nabla V \cdot \nabla + \beta^{-1} \Delta$ be the infinitesimal generator of $(X_t)_{t \geq 0}$ (satisfying (6)). Let us consider the first eigenvalue and eigenfunction associated with the adjoint operator $L^\dagger = \text{div}(\nabla V + \beta^{-1} \nabla)$ with homogeneous Dirichlet boundary condition on ∂S:

$$\begin{cases} L^\dagger u_1 = -\lambda_1 u_1 & \text{on } S, \\ u_1 = 0 & \text{on } \partial S. \end{cases} \qquad (12)$$

Then, the QSD ν_S associated with S satisfies

$$d\nu_S = \frac{u_1(x)\, dx}{\int_S u_1(x)\, dx}$$

where dx denotes the Lebesgue measure on S.

Notice that $L^\dagger$ is a negative operator in $L^2(e^{\beta V})$ so that $\lambda_1 > 0$. Moreover, it follows from general results on the first eigenfunction of elliptic operators that u_1 has a sign on S, so that one can choose without loss of generality $u_1 > 0$.

The QSD thus has a density with respect to Lebesgue measure, which is simply the ground state of the Fokker–Planck operator $L^\dagger$ associated with the dynamics with absorbing boundary conditions. This will be crucial in order to analyze the Eyring-Kramers formula in Section 4.

2.4 Third property: the exit event

Finally, the third property of the QSD concerns the exit event starting from the QSD. Let us assume that X_0 is distributed according to the QSD ν_S in S. Then the law of the pair (τ_S, X_{τ_S}) (the first exit time and the first exit point) is fully characterized by

the following properties: (i) τ_S is exponentially distributed with parameter λ_1 (defined in (12)); (ii) τ_S is independent of X_{τ_S}; (iii) The law of X_{τ_S} is the following: for any bounded measurable function $\varphi : \partial S \to \mathbb{R}$,

$$\mathbb{E}^{\nu_S}(\varphi(X_{\tau_S})) = -\frac{\int_{\partial S} \varphi \, \partial_n u_1 \, d\sigma}{\beta \lambda_1 \int_S u_1(x)\, dx}, \qquad (13)$$

where σ denotes the Lebesgue measure on ∂S and $\partial_n u_1 = \nabla u_1 \cdot n$ denotes the outward normal derivative of u_1 (defined in (12)) on ∂S. The superscript ν_S in $\mathbb{E}^{\nu_S}$ indicates that the initial condition X_0 is assumed to be distributed according to ν_S.

2.5 Error estimate on the exit event

We can now state a result concerning the error made when approximating the exit event of the process which remains for a long time in S by the exit event of the process starting from the QSD. The following result is proven in[46]. Let $(X_t)_{t \geq 0}$ satisfy (6) with $X_0 \in S$. Introduce the first two eigenvalues $-\lambda_2 < -\lambda_1 < 0$ of the operator $L^\dagger$ on S with homogeneous Dirichlet boundary conditions on ∂S (see Section 2.3). Then there exists a constant $C > 0$ (which depends on the law of X_0), such that, for all $t \geq \frac{C}{(\lambda_2 - \lambda_1)}$,

$$\|\mathscr{L}(\tau_S - t, X_{\tau_S} | \tau_S > t) - \mathscr{L}(\tau_S, X_{\tau_S} | X_0 \sim \nu_S)\|_{TV} \leq C e^{-(\lambda_2 - \lambda_1)t} \qquad (14)$$

where

$$\|\mathscr{L}(\tau_S - t, X_{\tau_S} | \tau_S > t) - \mathscr{L}(\tau_S, X_{\tau_S} | X_0 \sim \nu_S)\|_{TV}$$

$$= \sup_{f, \|f\|_{L^\infty} \leq 1} \left| \mathbb{E}(f(\tau_S - t, X_{\tau_S}) | \tau_S > t) - \mathbb{E}^{\nu_S}(f(\tau_S, X_{\tau_S})) \right|$$

denotes the total variation norm of the difference between the law of $(\tau_S - t, X_{\tau_S})$ conditioned to $\tau_S > t$ (for any initial condition $X_0 \in S$), and the law of (τ_S, X_{τ_S}) when X_0 is distributed according to ν_S. The supremum is taken over all bounded functions $f : \mathbb{R}_+ \times \partial S \to \mathbb{R}$, with L^∞-norm smaller than one.

This gives a way to quantify the local equilibration time mentioned in the introduction of Section 2, which is the typical time to get the convergence in (11): it is of order $1/(\lambda_2 - \lambda_1)$. Of course, this is not a very practical result since computing the eigenvalues λ_1 and λ_2 is in general impossible. We will discuss in Section 3.3 a practical way to estimate this time.

As a consequence, this result also gives us a way to define a metastable state: the local equilibration time is of order $1/(\lambda_2 - \lambda_1)$, the exit time is of order $1/\lambda_1$ and thus, the state S is metastable if

$$\frac{1}{\lambda_1} \gg \frac{1}{\lambda_2 - \lambda_1}. \qquad (15)$$

2.6 A first discussion on QSD and jump Markov model

Let us now go back to our discussion on the link between the overdamped Langevin dynamics (6) and the jump Markov dynamics (4). Using the first property 2.2, if the process remains in S for a long time, then it is approximately distributed according to the QSD, and the error can be quantified thanks to (14). There-

fore, to study the exit from S, it is relevant to consider a process starting from the QSD ν_S in S. Then, the third property 2.4 shows that the exit event can indeed be identified with one step of a Markov jump process since τ_S is exponentially distributed and independent of X_{τ_S}, which are the basic requirements of a move of a Markov jump process (see Section 1.1).

In other words, the QSD ν_S is the natural initial distribution to choose in a metastable state S in order to parametrize an underlying jump Markov model.

In order to be more precise, let us assume that the state S is surrounded by I neighboring states. The boundary ∂S is then divided into I disjoint subsets $(\partial S_i)_{i=1,\dots,I}$, each of them associated with an exit towards one of the neighboring states, which we assume to be numbered by $1,\dots,I$ without loss of generality: $\mathcal{N}_0 = \{1,\dots,I\}$ (see Figure 1 for a situation where $I = 4$). The exit event from S is characterized by the pair $(\tau_S, \mathcal{I})$, where $\mathcal{I}$ is a random variable which gives the next visited state:

$$\text{for } i = 1,\dots,I, \quad \{\mathcal{I} = i\} = \{X_{\tau_S} \in \partial S_i\}.$$

Notice that τ_S and $\mathcal{I}$ are by construction independent random variables. The jump Markov model is then parametrized as follows. Introduce (see Equation (13) for the exit point distribution)

$$p(i) = \mathbb{P}(X_{\tau_S} \in \partial S_i) = -\frac{\int_{\partial S_i} \partial_n u_1 \, d\sigma}{\beta \lambda_1 \int_S u_1(x) \, dx}, \quad \text{for } i = 1,\dots,I. \quad (16)$$

For each exit region ∂S_i, let us define the corresponding rate

$$\text{for } i = 1,\dots,I, \, k_{0,i} = \lambda_1 p(i). \quad (17)$$

Now, one can check that

- The exit time τ_S is exponentially distributed with parameter $\sum_{i \in \mathcal{N}_0} k_{0,i}$, in accordance with (2).
- The next visited state is $\mathcal{I}$, independent of τ_S and with law: for $j \in \mathcal{N}_0$, $\mathbb{P}(\mathcal{I} = j) = \frac{k_{0,j}}{\sum_{i \in \mathcal{N}_0} k_{0,i}}$, in accordance with (3).

Let us emphasize again that τ_S and X_{τ_S} are independent random variables, which is a crucial property to recover the Markov jump model (in (2)–(3), conditionally on Y_n, T_n and Y_{n+1} are indeed independent).

The rates given by (17) are exact, in the sense that starting from the QSD, the law of the exit event from S is exact using this definition for the transitions to neighboring states. In Section 4, we will discuss the error introduced when approximating these rates by the Eyring-Kramers formula (7).

As a comment on the way we define the rates, let us mention that in the original works by Kramers [14] (see also [48]), the idea is to introduce the stationary Fokker-Planck equation with zero boundary condition (sinks on the boundary of S) and with a source term within S (source in S), and to look at the steady state outgoing current on the boundary ∂S. When the process leaves S, it is reintroduced in S according to the source term. In general, the stationary state depends on the source term of course. The difference with the QSD approach (see (12)) is that we consider the first eigenvalue of the Fokker-Planck operator. This corresponds

to the following: when the process leaves S, it is reintroduced in S according to the empirical law along the path of the process in S. The interest of this point of view is that the exit time distribution is exactly exponential (and not approximately exponential in some small temperature or high barrier regime).

2.7 Concluding remarks

The interest of the QSD approach is that it is very general and versatile. The QSD can be defined for any stochastic process: reversible or non-reversible, with values in a discrete or a continous state space, etc, see [47]. Then, the properties that the exit time is exponentially distributed and independent of the exit point are satisfied in these very general situations.

Let us emphasize in particular that in the framework of the two dynamics (5) and (6) we consider here, the QSD gives a natural way to define rates to leave a metastable state, without any small temperature assumption. Moreover, the metastability may be related to either energetic barriers or entropic barriers (see in particular [49] for numerical experiments in purely entropic cases). Roughly speaking, energetic barriers correspond to a situation where it is difficult to leave S because it corresponds to the basin of attraction of a local minimum of V for the gradient dynamics $\dot{x} = -\nabla V(x)$: the process has to go over an energetic hurdle (namely a saddle point of V) to leave S. Entropic barriers are different. They appear when it takes time for the process to leave S because the exit doors from S are very narrow. The potential within S may be constant in this case. In practice, entropic barriers are related to steric constraints in the atomic system. The extreme case for an entropic barrier is a Brownian motion ($V = 0$) reflected on $\partial S \setminus \Gamma$, $\Gamma \subset \partial S$ being the small subset of ∂S through which the process can escape from S. For applications in biology for example, being able to handle both energetic and entropic barriers is important.

Let us note that the QSD in S is in general different from the Boltzmann distribution restricted to S: the QSD is zero on the boundary of ∂S while this is not the case for the Boltzmann distribution.

The remaining of the article is organized as follows. In Section 3, we review recent results which show how the QSD can be used to justify and analyze accelerated dynamics algorithms, and in particular the parallel replica algorithm. These techniques aim at efficiently sample the state-to-state dynamics associated with the microscopic models (5) and (6), using the underlying jump Markov model to accelerate the sampling of the exit event from metastable states. In Section 4, we present new results concerning the justification of the Eyring-Kramers formula (7) for parametrizing a jump Markov model. The two following sections are essentially independent of each other and can be read separately.

3 Numerical aspects: accelerated dynamics

As explained in the introduction, it is possible to use the underlying Markov jump process as a support to accelerate molecular dynamics. This is the principle of the accelerated dynamics methods

introduced by A.F. Voter in the late nineties[3–5]. These techniques aim at efficiently simulate the exit event from a metastable state.

Three ideas have been explored. In the parallel replica algorithm[4,50], the idea is to use the jump Markov model in order to parallelize the sampling of the exit event. The principle of the hyperdynamics algorithm[3] is to raise the potential within the metastable states in order to accelerate the exit event, while being able to recover the correct exit time and exit point distributions. Finally, the temperature accelerated dynamics[5] consists in simulating exit events at high temperature, and to extrapolate them at low temperature using the Eyring-Kramers law (7). In this paper, for the sake of conciseness, we concentrate on the analysis of the parallel replica method, and we refer to the papers[51,52] for an analysis of hyperdynamics and temperature accelerated dynamics. See also the recent review[44] for a detailed presentation.

3.1 The parallel replica method

In order to present the parallel replica method, we need to introduce a partition of the configuration space $\mathbb{R}^d$ to describe the states. Let us denote by

$$\mathscr{S} : \mathbb{R}^d \to \mathbb{N} \qquad (18)$$

a function which associates to a configuration $x \in \mathbb{R}^d$ a state number $\mathscr{S}(x)$. We will discuss below how to choose in practice this function $\mathscr{S}$. The aim of the parallel replica method (and actually also of hyperdynamics and temperature accelerated dynamics) is to generate very efficiently a trajectory $(S_t)_{t \geq 0}$ with values in $\mathbb{N}$ which has approximately the same law as the state-to-state dynamics $(\mathscr{S}(X_t))_{t \geq 0}$ where $(X_t)_{t \geq 0}$ follows (6). The states are the level sets of $\mathscr{S}$. Of course, in general, $(\mathscr{S}(X_t))_{t \geq 0}$ is not a Markov process, but it is close to Markovian if the level sets of $\mathscr{S}$ are metastable regions, see Sections 2.2 and 2.5. The idea is to check and then use metastability of the states in order to efficiently generate the exit events.

As explained above, we present for the sake of simplicity the algorithm in the setting of the overdamped Langevin dynamics (6), but the algorithm and the discussion below can be generalized to the Langevin dynamics (5), and actually to any Markov dynamics, as soon as a QSD can be defined in each state.

The parallel replica algorithm consists in iterating three steps:

- *The decorrelation step*: In this step, a reference replica evolves according to the original dynamics (6), until it remains trapped for a time t_{corr} in one of the states $\mathscr{S}^{-1}(\{n\}) = \{x \in \mathbb{R}^d, \mathscr{S}(x) = n\}$, for $n \in \mathbb{N}$. The parameter t_{corr} should be chosen by the user, and may depend on the state. During this step, no error is made, since the reference replica evolves following the original dynamics (and there is of course no computational gain compared to a naive direct numerical simulation). Once the reference replica has been trapped in one of the states (that we denote generically by S in the following two steps) for a time t_{corr}, the aim is to generate very efficiently the exit event. This is done in two steps.

- *The dephasing step*: In this preparation step, $(N-1)$ config-

urations are generated within S (in addition to the one obtained form the reference replica) as follows. Starting from the position of the reference replica at the end of the decorrelation step, some trajectories are simulated in parallel for a time t_{corr}. For each trajectory, if it remains within S over the time interval of length t_{corr}, then its end point is stored. Otherwise, the trajectory is discarded, and a new attempt to get a trajectory remaining in S for a time t_{corr} is made. This step is pure overhead. The objective is only to get N configurations in S which will be used as initial conditions in the parallel step.

- *The parallel step*: In the parallel step, N replicas are evolved independently and in parallel, starting from the initial conditions generated in the dephasing step, following the original dynamics (6) (with independent driving Brownian motions). This step ends as soon as one of the replica leaves S. Then, the simulation clock is updated by setting the residence time in the state S to N (the number of replicas) times the exit time of the first replica which left S. This replica now becomes the reference replica, and one goes back to the decorrelation step above.

The computational gain of this algorithm is in the parallel step, which (as explained below) simulates the exit event in a wall clock time N times smaller in average than what would be necessary to see the reference walker leaving S. This of course requires a parallel architecture able to handle N jobs in parallel[†]. This algorithm can be seen as a way to parallelize in time the simulation of the exit event, which is not trivial because of the sequential nature of time.

Before we present the mathematical analysis of this method, let us make a few comments on the choice of the function $\mathscr{S}$. In the original papers[4,50], the idea is to define states as the basins of attraction of the local minima of V for the gradient dynamics $\dot{x} = -\nabla V(x)$. In this context, it is important to notice that the states do not need to be defined *a priori*: they are numbered as the process evolves and discovers new regions (namely new local minima of V reached by the gradient descent). This way to define $\mathscr{S}$ is well suited for applications in material sciences, where barriers are essentially energetic barriers, and the local minima of V indeed correspond to different macroscopic states. In other applications, for example in biology, there may be too many local minima, not all of them being significant in terms of macroscopic states. In that case, one could think of using a few degrees of freedom (reaction coordinates) to define the states, see for example[53]. Actually, in the original work by Kramers[14], the states are also defined using reaction coordinates, see the discussion in[16]. The important outcome of the mathematical analysis below is that, whatever the choice of the states, if one is able to define a correct correlation time t_{corr} attached to the states, then the algorithm is consistent. We will discuss in Section 3.2 how large t_{corr} should be theoretically, and in Section 3.3 how to estimate it in

---

[†] For a discussion on the parallel efficiency, communication and synchronization, we refer to the papers[4,46,49,50].

practice.

Another important remark is that one actually does not need a partition of the configuration space to apply this algorithm. Indeed, the algorithm can be seen as an efficient way to simulate the exit event from a metastable state S. Therefore, the algorithm could be applied even if no partition of the state space is available, but only an ensemble of disjoint subsets of the configuration space. The algorithms could then be used to simulate efficiently exit events from these states, if the system happens to be trapped in one of them.

3.2 Mathematical analysis

Let us now analyze the parallel replica algorithm described above, using the notion of quasi-stationary distribution. In view of the first property 2.2 of the QSD, the decorrelation step is simply a way to decide wether or not the reference replica remains sufficiently long in one of the states so that it can be considered as being distributed according to the QSD. In view of (14), the error is of the order of $\exp(-(\lambda_2 - \lambda_1)t_{corr})$ so that t_{corr} should be chosen of the order of $1/(\lambda_2 - \lambda_1)$ in order for the exit event of the reference walker which remains in S for a time t_{corr} to be statistically close to the exit event generated starting from the QSD.

Using the same arguments, the dephasing step is nothing but a rejection algorithm to generate many configurations in S independently and identically distributed with law the QSD ν_S in S. Again, the distance to the QSD of the generated samples can be quantified using (14).

Finally, the parallel step generates an exit event which is exactly the one that would have been obtained considering only one replica. Indeed, up to the error quantified in (14), all the replica are i.i.d. with initial condition the QSD ν_S. Therefore, according to the third property 2.4 of the QSD, their exit times $(\tau_S^n)_{n \in \{1, \dots N\}}$ are i.i.d. with law an exponential distribution with parameter λ_1 (τ_S^n being the exit time of the n-th replica) so that

$$N \min_{n \in \{1, \dots, N\}} (\tau_S^n) \overset{\mathscr{L}}{=} \tau_S^1. \tag{19}$$

This explains why the exit time of the first replica which leaves S needs to be multiplied by the number of replicas N. This also shows why the parallel step gives a computational gain in terms of wall clock: the time required to simulate the exit event is divided by N compared to a direct numerical simulation. Moreover, since starting from the QSD, the exit time and the exit point are independent, we also have

$$X_{\tau_S^{I_0}}^{I_0} \overset{\mathscr{L}}{=} X_{\tau_S^1}^1,$$

where $(X_t^n)_{t \geq 0}$ is the n-th replica and $I_0 = \arg\min_{n \in \{1, \dots, N\}} (\tau_S^n)$ is the index of the first replica which exits S. The exit point of the first replica which exits S is statistically the same as the exit point of the reference walker. Finally, by the independence property of exit time and exit point, one can actually combine the two former results in a single equality in law on couples of random variables,

which shows that the parallel step is statistically exact:

$$\left(N \min_{n \in \{1, \dots, N\}} (\tau_S^n), X_{\tau_S^{I_0}}^{I_0}\right) \overset{\mathscr{L}}{=} (\tau_S^1, X_{\tau_S^1}^1).$$

As a remark, let us notice that in practice, discrete-time processes are used (since the Langevin or overdamped Langevin dynamics are discretized in time). Then, the exit times are not exponentially but geometrically distributed. It is however possible to generalize the formula (19) to this setting by using the following fact: if $(\sigma_n)_{n \in \{1, \dots N\}}$ are i.i.d. with geometric law, then $N(\min(\sigma_1, \dots, \sigma_N) - 1) + \min(n \in \{1, \dots, N\}, \sigma_n = \min(\sigma_1, \dots, \sigma_N)) \overset{\mathscr{L}}{=} \sigma_1$. We refer to [54] for more details.

This analysis shows that the parallel replica is a very versatile algorithm. In particular it applies to both energetic and entropic barriers, and does not assume a small temperature regime (in contrast with the analysis we will perform in Section 4). The only errors introduced in the algorithm are related to the rate of convergence to the QSD of the process conditioned to stay in the state. The algorithm will be efficient if the convergence time to the QSD is small compared to the exit time (in other words, if the states are metastable). Formula (14) gives a way to quantify the error introduced by the whole algorithm. In the limit $t_{corr} \to \infty$, the algorithm generates exactly the correct exit event. However, (14) is not very useful to choose t_{corr} in practice since it is not possible to get accurate estimates of λ_1 and λ_2 in general. We will present in the next section a practical way to estimate t_{corr}.

Let us emphasize that this analysis gives some error bound on the accuracy of the *state-to-state dynamics* generated by the parallel replica algorithm, and not only on the invariant measure, or the evolution of the time marginals.

3.3 Recent developments on the parallel replica algorithm

In view of the previous mathematical analysis, an important practical question is how to choose the correlation time t_{corr}. In the original papers [4,50], the correlation time is estimated assuming that an harmonic approximation is accurate. In [49], we propose another approach which could be applied in more general settings. The idea is to use two ingredients:

- The Fleming-Viot particle process [55], which consists in N replicas $(X_t^1, \dots, X_t^N)_{t \geq 0}$ which are evolving and interacting in such a way that the empirical distribution $\frac{1}{N} \sum_{n=1}^{N} \delta_{X_t^n}$ is close (in the large N limit) to the law of the process X_t conditioned on $t < \tau_S$.

- The Gelman-Rubin convergence diagnostic [56] to estimate the correlation time as the convergence time to a stationary state for the Fleming-Viot particle process.

Roughly speaking, the Fleming-Viot process consists in following the original dynamics (6) independently for each replica, and, each time one of the replicas leaves the domain S, another one taken at random is duplicated. The Gelman-Rubin convergence diagnostic consists in comparing the average of a given observable over replicas at a given time, with the average of this observ-

able over time and replicas: when the two averages are close (up to a tolerance, and for well chosen observables), the process is considered at stationarity.

Then, the generalized parallel replica algorithm introduced in[49] is a modification of the original algorithm where, each time the reference replica enters a new state, a Fleming-Viot particle process is launched using $(N-1)$ replicas simulated in parallel. Then the decorrelation step consists in the following: if the reference replica leaves S before the Fleming-Viot particle process reaches stationarity, then a new decorrelation step starts (and the replicas generated by the Fleming-Viot particle are discarded); if otherwise the Fleming-Viot particle process reaches stationarity before the reference replica leaves S, then one proceeds to the parallel step. Notice indeed that the final positions of the replicas simulated by the Fleming-Viot particle process can be used as initial conditions for the processes in the parallel step. This procedure thus avoids the choice of a t_{corr} *a priori*: it is in some sense estimated on the fly. For more details, discussions on the correlations included by the Fleming-Viot process between the replicas, and numerical experiments (in particular in cases with purely entropic barriers), we refer to[49].

3.4 Concluding remarks

We presented the results in the context of the overdamped Langevin dynamics (6), but the algorithms straightforwardly apply to any stochastic Markov dynamics as soon as a QSD exists (for example Langevin dynamics for a bounded domain, see[45]).

The QSD approach is also useful to analyze the two other accelerated dynamics: hyperdynamics[51] and temperature accelerated dynamics[52]. Typically, one expects better speed up with these algorithms than with parallel replica, but at the expense of larger errors and more stringent assumptions (typically energetic barriers, and small temperature regime), see[44] for a review paper. Let us mention in particular that the mathematical analysis of the temperature accelerated dynamics algorithms requires to prove that the distribution for the next visited state predicted using the Eyring-Kramers formula (7) is correct, as explained in[52]. The next section is thus also motivated by the development of an error analysis for temperature accelerated dynamics.

Let us finally mention that in these algorithms, the way to relate the original dynamics to a jump Markov process is by looking at $(\mathscr{S}(X_t))_{t\geq 0}$ (or $(\mathscr{S}(q_t))_{t\geq 0}$ for (5)). As already mentioned, this is not a Markov process, but it is close to Markovian if the level sets of $\mathscr{S}$ are metastable sets, see Sections 2.2 and 2.5. In particular, in the parallel replica algorithm above, the non-Markovian effects (and in particular the recrossing at the boundary between two states) are taken into account using the decorrelation step, where the exact process is used in these intermediate regimes between long sojourns in metastable states. As already mentioned above (see the discussion on the map $\mathscr{S}$ at the end of Section 3.1), another idea is to introduce an ensemble of disjoint subsets $(M_i)_{i\geq 0}$ and to project the dynamics $(X_t)_{t\geq 0}$ (or $(q_t)_{t\geq 0}$) onto a discrete state-space dynamics by considering *the last visited milestone*[35,57]. Notice that these subsets do not create a partition of the state space. They are sometimes called milestones[33], tar-

get sets or core sets[35] in the literature. The natural parametrization of the underlying jump process is then to consider, starting from a milestone (say M_0), the time to reach any of the other milestones $((M_j)_{j\neq 0})$ and the index of the next visited milestone. This requires us to study the reactive paths among the milestones, for which many techniques have been developed, as already presented in the introduction. Let us now discuss the Markovianity of the projected dynamics. On the one hand, in the limit of very small milestones[‡], the sequence of visited states (*i.e.* the skeleton of the projected process) is naturally Markovian (even though the transition time is not necessarily exponential), but the description of the underlying continuous state space dynamics is very poor (since the information of the last visited milestone is not very informative about the actual state of the system). On the other hand, taking larger milestones, the projected process is close to a Markov process under some metastability assumptions with respect to these milestones. We refer to[17,58,59] for a mathematical analysis.

4 Theoretical aspects: transition state theory and Eyring-Kramers formula

In this section, we explore some theoretical counterparts of the QSD approach to study metastable stochastic processes. We concentrate on the overdamped Langevin dynamics (5). The generalization of the mathematical approach presented below to the Langevin dynamics would require some extra work.

We would like to justify the procedure described in the introduction to build jump Markov models, and which consists in (see for example[1,7,60]): (i) looking for all local minima and saddle points separating the local minima of the function V; (ii) connecting two minima which can be linked by a path going through a single saddle point, and parametrizing a jump between these two minima using the rate given by the Eyring-Kramers formula (7). More precisely, we concentrate on the accuracy of the sampling of the exit event from a metastable state using the jump Markov model. The questions we ask are the following: if a set S containing a single local minimum of V is metastable for the dynamics (6) (see the discussion in Section 2.2 and formula (15)), is the exit event predicted by the jump Markov model built using the Eyring-Kramers formula correct? What is the error induced by this approximation?

As already explained in Section 2.6, if S is metastable, one can assume that the stochastic process $(X_t)_{t\geq 0}$ satisfying (6) starts under the QSD ν_S (the error being quantified by (14)) and then, the exit time is exponentially distributed and independent of the exit point. Thus, two fundamental properties of the jump Markov model are satisfied. It only remains to prove that the rates associated with the exit event for $(X_t)_{t\geq 0}$ (see formula (17)) can be accurately approximated by the Eyring-Kramers formulas (7). As will become clear below, the analysis holds for energetic barriers in the small temperature regime $\beta \to \infty$.

In this section, we only sketch the proofs of our results, which

---

[‡] One could think of one-dimensional overdamped Langevin dynamics, with milestones defined as points: in this case the sequence of visited points is Markovian.

are quite technical. For a more detailed presentation, we refer to[61].

4.1 A review of the literature

Before presenting our approach, let us discuss the mathematical results in the literature aiming at justifying the Eyring-Kramers rates. See also the review article[62].

Some authors adopt a global approach: they look at the spectrum associated with the infinitesimal generator of the dynamics on the whole configuration space, and they compute the small eigenvalues in the small temperature regime $\beta \to \infty$. It can be shown that there are exactly m small eigenvalues, m being the number of local minima of V, and that these eigenvalues satisfy the Eyring-Kramers law (7), with an energy barrier $V(z_k) - V(x_k)$. Here, the saddle point z_k attached to the local minimum x_k is defined by[§]

$$V(z_k) = \inf_{\gamma \in \mathscr{P}(x_i, B_i)} \sup_{t \in [0,1]} V(\gamma(t))$$

where $\mathscr{P}(x_i, B_i)$ denotes the set of continuous paths from $[0,1]$ to $\mathbb{R}^d$ such that $\gamma(0) = x_i$ and $\gamma(1) \in B_i$ with B_i the union of small balls around local minima lower in energy than x_i. For the dynamics (6), we refer for example to the work[63] based on semiclassical analysis results for Witten Laplacian and the articles[64–66] where a potential theoretic approach is adopted. In the latter results, a connexion is made between the small eigenvalues and mean transition times between metastable states. Let us also mention the earlier results[67,68]. For the dynamics (5), similar results are obtained in[69]. These spectral approaches give the cascade of relevant time scales to reach from a local minimum any other local minimum which is lower in energy. They do not give any information about the typical time scale to go from one local minimum to any other local minimum (say from the global minimum to the second lower minimum). These global approaches can be used to build jump Markov models using a Galerkin projection of the infinitesimal generator onto the first m eigenmodes, which gives an excellent approximation of the infinitesimal generator. This has been extensively investigated by Schütte[¶] and his collaborators[17], starting with the seminal work[70].

In this work, we are interested in a local approach, namely in the study of the exit event from a given metastable state S. In this framework, the most famous approach to analyze the exit event is the large deviation theory[6]. In the small temperature regime, large deviation results provide the exponential rates (7), but without the prefactors and without error bounds. It can also be proven that the exit time is exponentially distributed in this regime, see[71]. For the dynamics (6), a typical result on the exit point distribution is the following (see[6] Theorem 5.1): for all $S' \subset\subset S$, for any $\gamma > 0$, for any $\delta > 0$, there exists $\delta_0 \in (0, \delta]$ and

$\beta_0 > 0$ such that for all $\beta \geq \beta_0$, for all $x \in S'$ and for all $y \in \partial S$,

$$e^{-\beta(V(y) - V(z_1) + \gamma)} \leq \mathbb{P}^x(X_{\tau_S} \in \mathscr{V}_{\delta_0}(y)) \leq e^{-\beta(V(y) - V(z_1) - \gamma)} \quad (20)$$

where $\mathscr{V}_{\delta_0}(y)$ is a δ_0-neighborhood of y in ∂S. Besides, let us also mention formal approaches to study the exit time and the exit point distribution that have been proposed by Matkowsky, Schuss and collaborators in[48,72,73] and by Maier and Stein in[74], using formal expansions for singularly perturbed elliptic equations. Some of the results cited above actually consider more general dynamics than (6) (including (5)), see also[75] for a recent contribution in that direction. One of the interests of the large deviation approach is actually to be sufficiently robust to apply to rather general dynamics.

Finally, some authors prove the convergence to a jump Markov process using a rescaling in time. See for example[76] for a one-dimensional diffusion in a double well, and[77,78] for a similar problem in larger dimension. In[79], a rescaled in time diffusion process converges to a jump Markov process living on the global minima of the potential V, assuming they are separated by saddle points having the same heights.

There are thus many mathematical approaches to derive the Eyring-Kramers formula. In particular, a lot of works are devoted to the computation of the rate between two metastable states, but very few discuss the use of the combination of these rates to build a jump Markov model between metastable states. To the best of our knowledge, none of these works quantify rigorously the error introduced by the use of the Eyring-Kramers formulas and a jump Markov process to model the transition from one state to all the neighboring states. Our aim in this section is to present such a mathematical analysis, using local versions of the spectral approaches mentioned above. Our approach is local, justifies the Eyring-Kramers formula with the prefactors and provides error estimates. It uses techniques developed in particular in the previous works[80,81]. These results generalize the results in dimension 1 in Section 4 of[52].

4.2 Mathematical result

Let us consider the dynamics (6) with an initial condition distributed according to the QSD ν_S in a domain S. We assume the following:

- The domain S is an open smooth bounded domain in $\mathbb{R}^d$.

- The function $V : \bar{S} \to \mathbb{R}$ is a Morse function with a single critical point x_1. Moreover, $x_1 \in S$ and $V(x_1) = \min_{\bar{S}} V$.

- The normal derivative $\partial_n V$ is strictly positive on ∂S, and $V|_{\partial S}$ is a Morse function with local minima reached at $z_1, \ldots, z_I$ with $V(z_1) < V(z_2) < \ldots < V(z_I)$.

- The height of the barrier is large compared to the saddle points heights discrepancies: $V(z_1) - V(x_1) > V(z_I) - V(z_1)$.

- For all $i \in \{1, \ldots I\}$, consider $B_{z_i} \subset \partial S$ the basin of attraction for the dynamics in the boundary ∂S: $\dot{x} = -\nabla_T V(x)$ (where

---

[§] It is here implicitly assumed that the inf sup value is attained at a single saddle point z_k.

[¶] In fact, Schütte et al. look at the eigenvalues close to 1 for the so-called transfer operator $P_t = e^{tL}$ (for a well chosen lag time $t > 0$), which is equivalent to looking at the small positive eigenvalues of $-L$

$\nabla_T V$ denotes the tangential gradient of V along the boundary ∂S). Assume that

$$\inf_{z \in B_{z_i}^c} d_a(z, z_i) > V(z_I) - V(z_1) \tag{21}$$

where $B_{z_i}^c = \partial S \setminus B_{z_i}$.

Here, d_a is the Agmon distance:

$$d_a(x, y) = \inf_{\gamma \in \Gamma_{x,y}} \int_0^1 g(\gamma(t)) |\gamma'(t)| \, dt$$

where $g = \begin{cases} |\nabla V| \text{ in } S \\ |\nabla_T V| \text{ in } \partial S \end{cases}$, and the infimum is over the set $\Gamma_{x,y}$ of all piecewise C^1 paths $\gamma : [0,1] \to \overline{S}$ such that $\gamma(0) = x$ and $\gamma(1) = y$. The Agmon distance is useful in order to measure the decay of eigenfunctions away from critical points. These are the so-called semi-classical Agmon estimates, see [82,83].

Then, in the limit $\beta \to \infty$, the exit rate is (see also [80])

$$\lambda_1 = \sqrt{\frac{\beta}{2\pi}} \partial_n V(z_1) \frac{\sqrt{\det(\nabla^2 V)(x_1)}}{\sqrt{\det(\nabla^2 V_{|\partial S})(z_1)}} e^{-\beta(V(z_1) - V(x_1))} (1 + O(\beta^{-1})).$$

Moreover, for any open set Σ_i containing z_i such that $\overline{\Sigma}_i \subset B_{z_i}$,

$$\frac{\int_{\Sigma_i} \partial_n u_1 \, d\sigma}{\int_S u_1(x) \, dx} = -A_i(\beta) e^{-\beta(V(z_i) - V(x_1))} (1 + O(\beta^{-1})), \tag{22}$$

where

$$A_i(\beta) = \frac{\beta^{3/2}}{\sqrt{2\pi}} \partial_n V(z_i) \frac{\sqrt{\det(\nabla^2 V)(x_1)}}{\sqrt{\det(\nabla^2 V_{|\partial S})(z_i)}}.$$

Therefore,

$$p(i) = \mathbb{P}^{\nu_S}(X_{\tau_S} \in \Sigma_i)$$

$$= \frac{\partial_n V(z_i) \sqrt{\det(\nabla^2 V_{|\partial S})(z_1)}}{\partial_n V(z_1) \sqrt{\det(\nabla^2 V_{|\partial S})(z_i)}} e^{-\beta(V(z_i) - V(z_1))} (1 + O(\beta^{-1}))$$

$$\tag{23}$$

and (see Equation (17) for the definition of the exit rates)

$$k_{0,i} = \lambda_1 p(i)$$

$$= \widetilde{v}_{0,i}^{OL} e^{-\beta(V(z_i) - V(x_1))} (1 + O(\beta^{-1})) \tag{24}$$

where the prefactors $\widetilde{v}_{0,i}^{OL}$ are given by

$$\widetilde{v}_{0,i}^{OL} = \sqrt{\frac{\beta}{2\pi}} \partial_n V(z_i) \frac{\sqrt{\det(\nabla^2 V)(x_1)}}{\sqrt{\det(\nabla^2 V_{|\partial S})(z_i)}}. \tag{25}$$

We refer to [61] for more details, and other related results.

As stated in the assumptions, these rates are obtained assuming $\partial_n V > 0$ on ∂S: the local minima $z_1, \ldots, z_I$ of V on ∂S are therefore not saddle points of V but so-called *generalized saddle points* (see [80,81]). In a future work, we intend to extend these results to

the case where the points $(z_i)_{1 \le i \le I}$ are saddle points of V, in which case we expect to prove the same result (24) for the exit rates, with the prefactor $\widetilde{v}_{0,i}^{OL}$ being $\frac{1}{\pi} |\lambda^-(z_j)| \frac{\sqrt{\det(\nabla^2 V)(x_1)}}{\sqrt{|\det(\nabla^2 V)(z_j)|}}$ (this formula can be obtained using formal expansions on the exit time and the Laplace's method). Notice that the latter formula differs from (9) by a multiplicative factor $1/2$ since λ_1 is the exit rate from S and not the transition rate to one of the neighboring state (see the remark on page 408 in [64] on this multiplicative factor $1/2$ and the results on asymptotic exit times in [74] for example). This factor is due to the fact that once on the saddle point, the process has a probability one half to go back to S, and a probability one half to effectively leave S. This multiplicative factor does not have any influence on the law of the next visited state which only involves ratio of the rates $k_{0,i}$, see Equation (3).

4.3 Discussion of the result

As already discussed above, the interest of these results is that they justify the use of the Eyring-Kramers formula to model the exit event using a jump Markov model. They give in particular the relative probability to leave S through each of the local minima z_i of V on the boundary ∂S. Moreover, we obtain an estimate of the relative error on the exit probabilities (and not only on the logarithm of the exit probabilities as in (20)): it is of order β^{-1}, see Equation (23).

The importance of obtaining a result including the prefactors in the rates is illustrated by the following result, which is also proven in [61]. Consider a simple situation with only two local minima z_1 and z_2 on the boundary (with as above $V(z_1) < V(z_2)$). Compare the two exit probabilities:

- The probability to leave through Σ_2 such that $\overline{\Sigma_2} \subset B_{z_2}$ and $z_2 \in \Sigma_2$;

- The probability to leave through Σ such that $\overline{\Sigma} \subset B_{z_1}$ and $\inf_\Sigma V = V(z_2)$.

By classical results from the large deviation theory (see for example (20)) the probability to exit through Σ and Σ_2 both scale like a prefactor times $e^{-\beta(V(z_2) - V(z_1))}$: the difference can only be read from the prefactors. Actually, it can be proven that, in the limit $\beta \to \infty$,

$$\frac{\mathbb{P}^{\nu_S}(X_{\tau_S} \in \Sigma)}{\mathbb{P}^{\nu_S}(X_{\tau_S} \in \Sigma_2)} = O(\beta^{-1/2}).$$

The probability to leave through Σ_2 (namely through the generalized saddle point z_2) is thus much larger than through Σ, even though the two regions are at the same height. This result explains why the local minima of V on the boundary (namely the generalized saddle points) play such an important role when studying the exit event.

4.4 Sketch of the proof

In view of the formulas (16) and (17), we would like to identify the asymptotic behavior of the small eigenvalue λ_1 and of the normal derivative $\partial_n u_1$ on ∂S in the limit $\beta \to \infty$. We recall that (λ_1, u_1) are defined by the eigenvalue problem (12). In order to

work in the classical setting for Witten Laplacians, we make a unitary transformation of the original eigenvalue problem. Let us consider $v_1 = u_1 \exp(\beta V)$, so that

$$\begin{cases} L^{(0)} v_1 = -\lambda_1 v_1 \text{ on } S, \\ v_1 = 0 \text{ on } \partial S, \end{cases} \tag{26}$$

where $L^{(0)} = \beta^{-1}\Delta - \nabla V \cdot \nabla$ is a self adjoint operator on $L^2(\exp(-\beta V))$. We would like to study, in the small temperature regime $\partial_n u_1 = \partial_n v_1 e^{-\beta V}$ on ∂S (since $u_1 = 0$ on ∂S). Now, observe that ∇v_1 satisfies

$$\begin{cases} L^{(1)} \nabla v_1 = -\lambda_1 \nabla v_1 \text{ on } S, \\ \nabla_T v_1 = 0 \text{ on } \partial S, \\ (\beta^{-1}\text{div} - \nabla V \cdot)\nabla v_1 = 0 \text{ on } \partial S, \end{cases} \tag{27}$$

where

$$L^{(1)} = \beta^{-1}\Delta - \nabla V \cdot \nabla - \text{Hess}(V)$$

is an operator acting on 1-forms (namely on vector fields). Therefore ∇v_1 is an eigenvector (or an eigen-1-form) of the operator $-L^{(1)}$ with tangential Dirichlet boundary conditions (see (27)), associated with the small eigenvalue λ_1. It is known (see for example[80]) that in our geometric setting $-L^{(0)}$ admits exactly one eigenvalue smaller than $\beta^{-1/2}$, namely λ_1 with associated eigenfunction v_1 (this is because V has only one local minimum in S) and that $-L^{(1)}$ admits exactly I eigenvalues smaller than $\beta^{-1/2}$ (where, we recall, I is the number of local minima of V on ∂S). Actually, all these small eigenvalues are exponentially small in the regime $\beta \to \infty$, the larger eigenvalues being bounded from below by a constant in this regime. The idea is then to construct an appropriate basis (with eigenvectors localized on the generalized saddle points, see the quasi-modes below) of the eigenspace associated with small eigenvalues for $L^{(1)}$, and then to decompose ∇v_1 along this basis.

The second step (the most technical one actually) is to build so-called *quasi-modes* which approximate the eigenvectors of $L^{(0)}$ and $L^{(1)}$ associated with small eigenvalues in the regime $\beta \to \infty$. A good approximation of v_1 is actually simply $\tilde{v} = Z\chi_{S'}$ where S' is an open set such that $\overline{S'} \subset S$, $\chi_{S'}$ is a smooth function with compact support in S and equal to one on S', and Z is a normalization constant such that $\|\tilde{v}\|_{L^2(e^{-\beta V})} = 1$. The difficult part is to build an approximation of the eigenspace $\text{Ran}\left(1_{[0,\beta^{-1/2}]}(-L^{(1)})\right)$, where $1_{[0,\beta^{-1/2}]}(-L^{(1)})$ denotes the spectral projection of $(-L^{(1)})$ over eigenvectors associated with eigenvalues in the interval $[0,\beta^{-1/2}]$. Using auxiliary simpler eigenvalue problems and WKB expansions around each of the local minima $(z_i)_{i=1,\dots,I}$, we are able to build 1-forms $(\psi_i)_{i=1,\dots,I}$ such that $\text{Span}(\psi_1,\dots,\psi_I)$ is a good approximation of $\text{Ran}\left(1_{[0,\beta^{-1/2}]}(-L^{(1)})\right)$. The support of ψ_i is essentially in a neighborhood of z_i and Agmon estimates are used to prove exponential decay away from z_i.

The third step consists in projecting the approximation of ∇v_1 on the approximation of the eigenspace $\text{Ran}\left(1_{[0,\beta^{-1/2}]}(-L^{(1)})\right)$ using the following result. Assume the following on the quasi-

modes:

- *Normalization:* $\tilde{v} \in H_0^1(e^{-\beta V})$ and $\|\tilde{v}\|_{L^2(e^{-\beta V})} = 1$. For all $i \in \{1,\dots,I\}$, $\psi_i \in H_T^1(e^{-\beta V})$ and $\| \|\psi_i\|_{L^2(e^{-\beta V})} = 1$.

- *Good quasi-modes:*

  - $\forall \delta > 0, \|\nabla\tilde{v}\|^2_{L^2(e^{-\beta V})} = O(e^{-\beta(V(z_1)-V(x_1)-\delta)})$,

  - $\exists \varepsilon > 0, \forall i \in \{1,\dots,I\}, \|1_{[\beta^{-1/2},\infty)}(-L^{(1)})\psi_i\|^2_{H^1(e^{-\beta V})} = O(e^{-\beta(V(z_I)-V(z_1)+\varepsilon)})$

- *Orthonormality of quasi-modes:* $\exists \varepsilon_0 > 0, \forall i < j \in \{1,\dots,I\}$,

  $$\langle \psi_i, \psi_j \rangle_{L^2(e^{-\beta V})} = O\left(e^{-\frac{\beta}{2}(V(z_j)-V(z_i)+\varepsilon_0)}\right).$$

- *Decomposition of $\nabla\tilde{v}$:* $\exists(C_i)_{1\leq i \leq I} \in \mathbb{R}^I, \exists p > 0, \forall i \in \{1,\dots,I\}$,

  $$\langle \nabla\tilde{v}, \psi_i \rangle_{L^2(e^{-\beta V})} = C_i \, \beta^{-p} e^{-\frac{\beta}{2}(V(z_i)-V(x_1))} \, (1 + O(\beta^{-1})).$$

- *Normal components of the quasi-modes:* $\exists(B_i)_{1\leq i \leq I} \in \mathbb{R}^I, \exists m > 0, \forall i,j \in \{1,\dots,I\}$,

  $$\int_{\Sigma_i} \psi_j \cdot n \, e^{-\beta V} d\sigma = \begin{cases} B_i \, \beta^{-m} \, e^{-\frac{\beta}{2}V(z_i)} \, (1 + O(\beta^{-1})) & \text{if } i = j, \\ 0 & \text{if } i \neq j. \end{cases}$$

Then for $i = 1,\dots,n$, when $\beta \to \infty$

$$\int_{\Sigma_i} \partial_n v_1 \, e^{-\beta V} d\sigma = C_i B_i \, \beta^{-(p+m)} \, e^{-\frac{\beta}{2}(2V(z_i)-V(x_1))} \, (1 + O(\beta^{-1})).$$

The proof is based on a Gram-Schmidt orthonormalization procedure. This result applied to the quasi-modes built in the second step yields (22).

4.5 On the geometric assumption (21)

In this section, we would like to discuss the geometric assumption (21). The question we would like to address is the following: is such an assumption necessary to indeed prove the result on the exit point density?

In order to test this assumption numerically, we consider the following simple two-dimensional setting. The potential function is $V(x,y) = x^2 + y^2 - ax$ with $a \in (0,1/9)$ on the domain S represented on Figure 2. The two local minima on ∂S are $z_1 = (1,0)$ and $z_2 = (-1,0)$. Notice that $V(z_2) - V(z_1) = 2a > 0$. The subset of the boundary around the highest saddle point is the segment Σ_2 joining the two points $(-1,-1)$ and $(-1,1)$. Using simple lower bounds on the Agmon distance, one can check that all the above assumptions are satisfied in this situation.

We then plot on Figures 3 ($a = 1/10$) and 4 ($a = 1/20$) the numerically estimated probability $f(\beta) = \mathbb{P}^{\nu_S}(X_{\tau_S} \in \Sigma_2)$, and compare it with the theoretical result $g(\beta) = \frac{\partial_n V(z_2)\sqrt{\det(\nabla^2 V|_{\partial S})(z_1)}}{\partial_n V(z_1)\sqrt{\det(\nabla^2 V|_{\partial S})(z_2)}} e^{-\beta(V(z_2)-V(z_1))}$ (see Equation (23)). The

---

$\|$ The functional space $H_T^1(e^{-\beta V})$ is the space of 1-forms in $H^1(e^{-\beta V})$ which satisfy the tangential Dirichlet boundary condition, see (27).
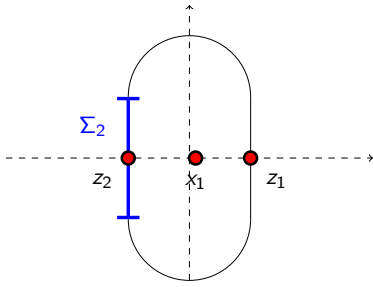
Fig. 2 The domain S is built as the union of the square with corners $(-1,-1)$ and $(1,1)$ and two half disks of radius 1 and with centers $(0,1)$ and $(0,-1)$.

probability $\mathbb{P}^{\nu_S}(X_{\tau_S} \in \Sigma_2)$ is estimated using a Monte Carlo procedure, and the dynamics (5) is discretized in time using an Euler-Maruyama scheme with timestep Δt. We observe an excellent agreement between the theory and the numerical results.
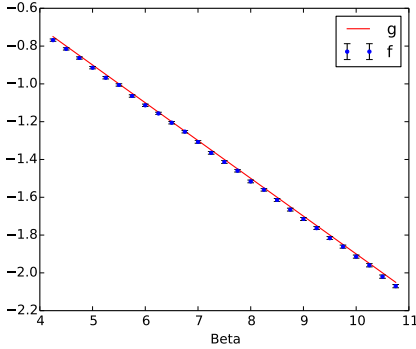

Fig. 3 The probability $\mathbb{P}^{\nu_S}(X_{\tau_S} \in \Sigma_2)$: comparison of the theoretical result (g) with the numerical result $(f, \Delta t = 5.10^{-3})$; $a = 1/10$.

Now, we modify the potential function V in order not to satisfy assumption (21) anymore. More precisely, the potential function is $V(x,y) = (y^2 - 2\,a(x))^3$ with $a(x) = a_1 x^2 + b_1 x + 0.5$ where a_1 and b_1 are chosen such that $a(-1+\delta) = 0$, $a(1) = 1/4$ for $\delta = 0.05$. We have $V(z_1) = -1/8$ and $V(z_2) = -8(a(-1))^3 > 0 > V(z_1)$. Moreover, two 'corniches' (which are in the level set $V^{-1}(\{0\})$ of V, and on which $|\nabla V| = 0$) on the 'slopes of the hills' of the potential V join the point $(-1+\delta, 0)$ to $B^c_{z_2}$ so that $\inf_{z \in B^c_{z_2}} d_a(z, z_2) < V(z_2) - V(z_1)$ (the assumption (21) is not satisfied). In addition $V|_{\partial S}$ is a Morse function. The function V is not a Morse function on S, but an arbitrarily small perturbation (which we neglect here) turns it into a Morse function. When comparing the numerically estimated probability $f(\beta) = \mathbb{P}^{\nu_S}(X_{\tau_S} \in \Sigma_2)$, with the theoretical result $g(\beta)$, we observe a discrepancy on the prefactors, see Figure 5.

Therefore, it seems that the construction of a jump Markov process using the Eyring-Kramers law to estimate the rates to the neighboring states is correct under some geometric assumptions. These geometric assumptions appear in the proof when estimating rigorously the accuracy of the WKB expansions as approximations of the quasi-modes of $L^{(1)}$.
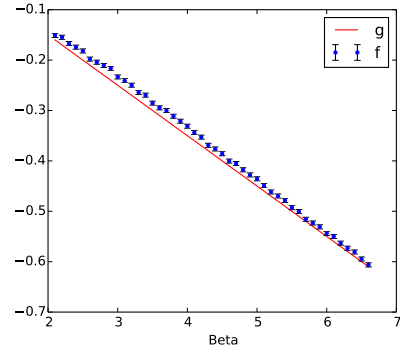

Fig. 4 The probability $\mathbb{P}^{\nu_S}(X_{\tau_S} \in \Sigma_2)$: comparison of the theoretical result (g) with the numerical result $(f, \Delta t = 2.10^{-3})$; $a = 1/20$.
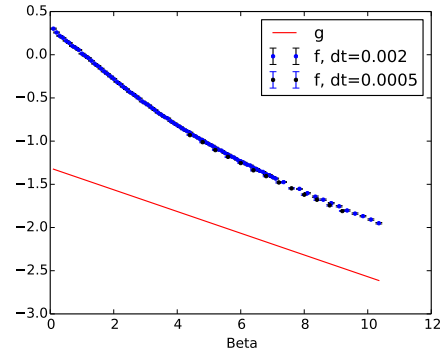

Fig. 5 The probability $\mathbb{P}^{\nu_S}(X_{\tau_S} \in \Sigma_2)$: comparison of the theoretical result (g) with the numerical result $(f, \Delta t = 2.10^{-3}$ and $\Delta t = 5.10^{-4})$.

4.6 Concluding remarks

In this section, we reported about some recent results obtained in[61]. We have shown that, under some geometric assumptions, the exit distribution from a state (namely the law of the next visited state) predicted by a jump Markov process built using the Eyring-Kramers formula is correct in the small temperature regime, if the process starts from the QSD in the state. We recall that this is a sensible assumption if the state is metastable, and Equation (14) gives a quantification of the error associated with this assumption. Moreover, we have obtained bounds on the error introduced by using the Eyring-Kramers formula.

The analysis shows the importance of considering (possibly generalized) saddle points on the boundary to identify the support of the exit point distribution. This follows from the precise estimates we obtain, which include the prefactor in the estimate of the probability to exit through a given subset of the boundary.

Finally, we checked by numerical experiments the fact that some geometric assumptions are indeed required in order for all these results to hold. These assumptions appear in the mathematical analysis when rigorously justifying WKB expansions.

As mentioned above, we intend to generalize the results to the case when the local minima of V on ∂S are saddle points.

References

1 A. Voter, in *Radiation Effects in Solids*, Springer, NATO Publishing Unit, 2005, ch. Introduction to the Kinetic Monte Carlo Method.

2 G. Bowman, V. Pande and F. Noé, *An Introduction to Markov State Models and Their Application to Long Timescale Molecular Simulation*, Springer, 2014.

3 A. Voter, *J. Chem. Phys.*, 1997, **106**, 4665–4677.

4 A. Voter, *Phys. Rev. B*, 1998, **57**, R13 985.

5 M. Sorensen and A. Voter, *J. Chem. Phys.*, 2000, **112**, 9599–9606.

6 M. Freidlin and A. Wentzell, *Random Perturbations of Dynamical Systems*, Springer-Verlag, 1984.

7 D. Wales, *Energy landscapes*, Cambridge University Press, 2003.

8 M. Cameron, *J. Chem. Phys.*, 2014, **141**, 184113.

9 R. Marcelin, *Ann. Physique*, 1915, **3**, 120–231.

10 M. Polanyi and H. Eyring, *Z. Phys. Chem. B*, 1931, **12**, 279.

11 H. Eyring, *Chemical Reviews*, 1935, **17**, 65–77.

12 E. Wigner, *Transactions of the Faraday Society*, 1938, **34**, 29–41.

13 J. Horiuti, *Bull. Chem. Soc. Japan*, 1938, **13**, 210–216.

14 H. Kramers, *Physica*, 1940, **7**, 284–304.

15 G. Vineyard, *Journal of Physics and Chemistry of Solids*, 1957, **3**, 121–127.

16 P. Hänggi, P. Talkner and M. Borkovec, *Reviews of Modern Physics*, 1990, **62**, 251–342.

17 M. Sarich and C. Schütte, *Metastability and Markov state models in molecular dynamics*, American Mathematical Society, 2013, vol. 24.

18 T. Lelièvre, M. Rousset and G. Stoltz, *Free energy computations: A mathematical perspective*, Imperial College Press, 2010.

19 G. Henkelman, G. Jóhannesson and H. Jónsson, in *Theoretical Methods in Condensed Phase Chemistry*, Springer, 2002, pp. 269–302.

20 W. E and E. Vanden-Eijnden, *Annual review of physical chemistry*, 2010, **61**, 391–420.

21 H. Jónsson, G. Mills and K. Jacobsen, in *Classical and Quantum Dynamics in Condensed Phase Simulations*, World Scientific, 1998, ch. Nudged Elastic Band Method for Finding Minimum Energy Paths of Transitions, pp. 385–404.

22 W. E, W. Ren and E. Vanden-Eijnden, *Phys. Rev. B*, 2002, **66**, 052301.

23 W. E, W. Ren and E. Vanden-Eijnden, *J. Phys. Chem. B*, 2005, **109**, 6688–6693.

24 R. Zhao, J. Shen and R. Skeel, *Journal of Chemical Theory and Computation*, 2010, **6**, 2411–2423.

25 C. Dellago, P. Bolhuis and D. Chandler, *J. Chem. Phys*, 1999, **110**, 6617–6625.

26 C. Dellago and P. Bolhuis, in *Advances computer simulation approaches for soft matter sciences I II*, Springer, 2009, vol. 221, pp. 167–233.

27 F. Cérou and A. Guyader, *Stoch. Anal. Appl.*, 2007, **25**, 417–443.

28 F. Cérou, A. Guyader, T. Lelièvre and D. Pommier, *J. Chem. Phys.*, 2011, **134**, 054108.

29 T. van Erp, D. Moroni and P. Bolhuis, *J. Chem. Phys.*, 2003, **118**, 7762–7774.

30 T. van Erp and P. Bolhuis, *J. Comp. Phys.*, 2005, **205**, 157–181.

31 R. Allen, P. Warren and P. ten Wolde, *Phys. Rev. Lett.*, 2005, **94**, 018104.

32 R. Allen, C. Valeriani and P. ten Wolde, *J. Phys.-Condens. Mat.*, 2009, **21**, 463102.

33 A. Faradjian and R. Elber, *J. Chem. Phys.*, 2004, **120**, 10880–10889.

34 L. Maragliano, E. Vanden-Eijnden and B. Roux, *J. Chem. Theory Comput.*, 2009, **5**, 2589–2594.

35 C. Schütte, F. Noé, J. Lu, M. Sarich and E. Vanden-Eijnden, *J. Chem. Phys.*, 2011, **134**, 204105.

36 W. E and E. Vanden-Eijnden, in *Multiscale modelling and simulation*, Springer, Berlin, 2004, vol. 39, pp. 35–68.

37 E. Vanden-Eijnden, M. Venturoli, G. Ciccotti and R. Elber, *J. Chem. Phys.*, 2008, **129**, 174102.

38 J. Lu and J. Nolen, *Probability Theory and Related Fields*, 2015, **161**, 195–244.

39 G. Henkelman and H. Jónsson, *J. Chem. Phys.*, 1999, **111**, 7010–7022.

40 J. Zhang and Q. Du, *SIAM J. Numer. Anal.*, 2012, **50**, 1899–1921.

41 G. Barkema and N. Mousseau, *Phys. Rev. Lett.*, 1996, **77**, 4358–4361.

42 N. Mousseau and G. Barkema, *Phys. Rev. E*, 1998, **57**, 2419–2424.

43 A. Samanta and W. E., *J. Chem. Phys.*, 2012, **136**, 124104.

44 T. Lelièvre, *Eur. Phys. J. Special Topics*, 2015, **224**, 2429–2444.

45 F. Nier, *Boundary conditions and subelliptic estimates for geometric Kramers-Fokker-Planck operators on manifolds with boundaries*, 2014, http://arxiv.org/abs/1309.5070.

46 C. Le Bris, T. Lelièvre, M. Luskin and D. Perez, *Monte Carlo Methods Appl.*, 2012, **18**, 119–146.

47 P. Collet, S. Martínez and J. San Martín, *Quasi-Stationary Distributions*, Springer, 2013.

48 T. Naeh, M. Klosek, B. Matkowsky and Z. Schuss, *SIAM J. Appl. Math.*, 1990, **50**, 595–627.

49 A. Binder, G. Simpson and T. Lelièvre, *J. Comput. Phys.*, 2015, **284**, 595–616.

50 D. Perez, B. Uberuaga and A. Voter, *Computational Materials Science*, 2015, **100**, 90–103.

51 T. Lelièvre and F. Nier, *Analysis & PDE*, 2015, **8**, 561–628.

52 D. Aristoff and T. Lelièvre, *SIAM Multiscale Modeling and Simulation*, 2014, **12**, 290–317.

53 O. Kum, B. Dickson, S. Stuart, B. Uberuaga and A. Voter, *J. Chem. Phys.*, 2004, **121**, 9808–9819.

54 D. Aristoff, T. Lelièvre and G. Simpson, *AMRX*, 2014, **2**, 332–

352.

55 P. Ferrari and N. Maric, *Electron. J. Probab.*, 2007, **12**, 684–702.

56 A. Gelman and D. Rubin, *Stat. Sci.*, 1992, **7**, 457–472.

57 N. Buchete and G. Hummer, *Phys. Rev. E*, 2008, **77**, 030902.

58 M. Sarich, F. Noé and C. Schütte, *Multiscale Model. Simul.*, 2010, **8**, 1154–1177.

59 A. Bovier and F. den Hollander, *Metastability, a potential theoretic approach*, Springer, 2015.

60 M. Cameron, *Netw. Heterog. Media*, 2014, **9**, 383–416.

61 G. Di Gesù, D. Le Peutrec, T. Lelièvre and B. Nectoux, *Precise asymptotics of the first exit point density for a diffusion process*, 2016, In preparation.

62 N. Berglund, *Markov Processes Relat. Fields*, 2013, **19**, 459–490.

63 B. Helffer, M. Klein and F. Nier, *Mat. Contemp.*, 2004, **26**, 41–85.

64 A. Bovier, M. Eckhoff, V. Gayrard and M. Klein, *J. Eur. Math. Soc. (JEMS)*, 2004, **6**, 399–424.

65 A. Bovier, V. Gayrard and M. Klein, *J. Eur. Math. Soc. (JEMS)*, 2005, **7**, 69–99.

66 M. Eckhoff, *Ann. Probab.*, 2005, **33**, 244–299.

67 L. Miclo, *Bulletin des sciences mathématiques*, 1995, **119**, 529–554.

68 R. Holley, S. Kusuoka and D. Stroock, *J. Funct. Anal.*, 1989, **83**, 333–347.

69 F. Hérau, M. Hitrik and J. Sjöstrand, *J. Inst. Math. Jussieu*, 2011, **10**, 567–634.

70 C. Schütte, *Conformational dynamics: modelling, theory, algorithm and application to biomolecules*, 1998, Habilitation dissertation, Free University Berlin.

71 M. Day, *Stochastics*, 1983, **8**, 297–323.

72 B. Matkowsky and Z. Schuss, *SIAM J. Appl. Math.*, 1977, **33**, 365–382.

73 Z. Schuss, *Theory and applications of stochastic processes: an analytical approach*, Springer, 2009, vol. 170.

74 R. S. Maier and D. L. Stein, *Phys. Rev. E*, 1993, **48**, 931–938.

75 F. Bouchet and J. Reygner, *Generalisation of the Eyring-Kramers transition rate formula to irreversible diffusion processes*, 2015, http://arxiv.org/abs/1507.02104.

76 C. Kipnis and C. Newman, *SIAM J. Appl. Math.*, 1985, **45**, 972–982.

77 A. Galves, E. Olivieri and M. E. Vares, *The Annals of Probability*, 1987, 1288–1305.

78 P. Mathieu, *Stochastics*, 1995, **55**, 1–20.

79 M. Sugiura, *Journal of the Mathematical Society of Japan*, 1995, **47**, 755–788.

80 B. Helffer and F. Nier, *Mémoire de la Société mathématique de France*, 2006, 1–89.

81 D. Le Peutrec, *Ann. Fac. Sci. Toulouse Math. (6)*, 2010, **19**, 735–809.

82 B. Simon, *Ann. of Math.*, 1984, 89–118.

83 B. Helffer and J. Sjöstrand, *Comm. Partial Differential Equations*, 1984, **9**, 337–408.